3-D Physical modeling study of a lower Cretaceous channel in central Alberta

Kelly D. Hrabi and Don C. Lawton

ABSTRACT

A physical model was constructed of a Lower Cretaceous meandering channel system from south central Alberta. Numerous 3-D acquisition tests were tried and it was found that receiver patch size has a significant effect on subsurface fold coverage and distribution.

A 2-D seismic line was shot over the model and it indicated that there is no significant variation in reflection amplitude strength from the point bar as it varies in thickness from 0-30 m. Sideswipe energy appears to mask any amplitude variation. The point bar appears to attenuate high frequencies and this produces a shadow zone under the point bar on deeper reflectors. Three post-stack time-migration algorithms were tested and each produced similar migrated sections but the running time of each algorithm varied significantly.

INTRODUCTION

Seismic modeling has been used to increase our understanding of complexities that occur on seismic data as well as to gain insight into the seismic signature that specific physical situations produce.

A physical seismic model was produced of a Lower Cretaceous meandering channel system from south central Alberta. Various 3-D acquisition schemes were tested using Seismic Image Software's FD33 package. A 2-D high resolution and a full 3-D seismic survey where acquired over this model using the University of Calgary's physical modeling tank. The 2-D data set is completely processed and three different post-stack time-migration algorithms were applied to the data set. The 3-D data set is currently been processed and it is presently at the velocity analysis stage of processing The 3-D data set is being processed for AVO analysis to see if 3-D AVO is a viable option for identification and interpretation of point bars in a meandering stream environment.

GEOLOGICAL SETTING

The geology of the Little Bow area of southern Alberta T 14 R 18-19W4 has been extensively studied by Hopkins (et al, 1982) and Wood (et al, 1989). This area is also of interest to the petroleum industry due to the discovery of oil in valley fill channels of the Glaconitic Member of the Upper Manniville formation (Hopkins et al, 1982). A informal stratigraphic column of the Lower Cretaceous group in the study area is shown in Figure 1. The Upper Manniville A, B, and C Divisions were given the nomenclature Manniville for this study.

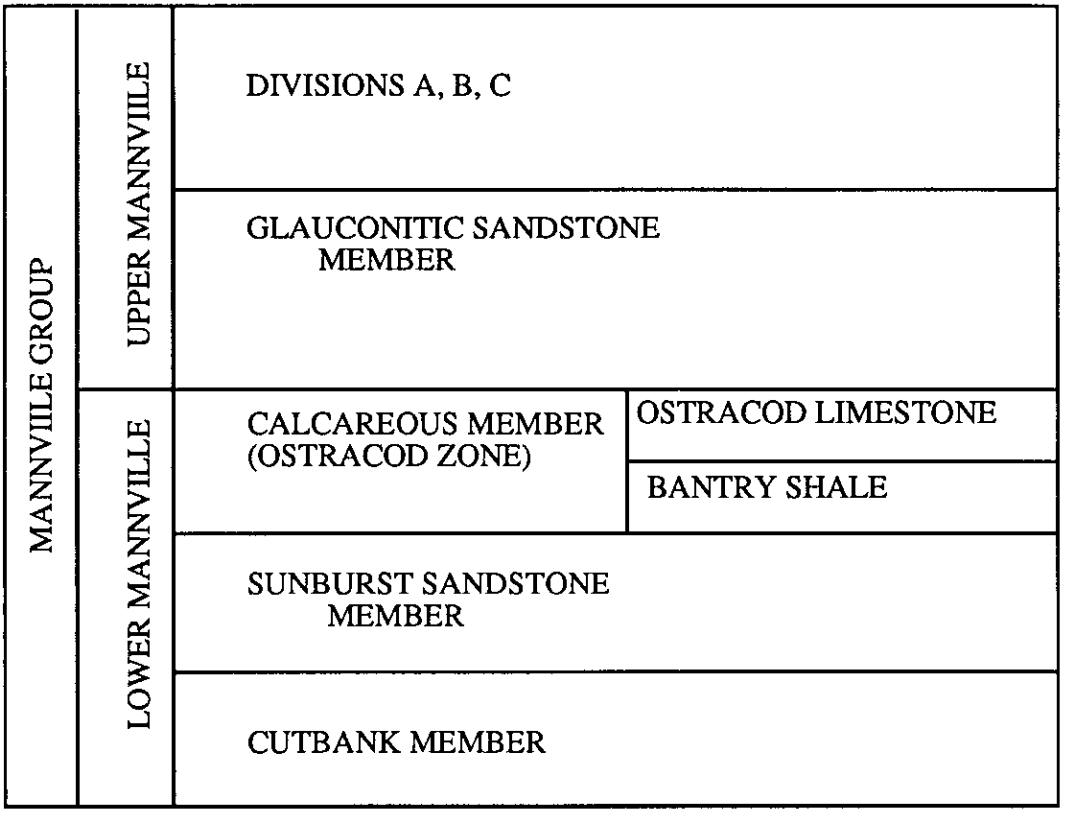

FIG. 1. Informal stratigraphic column for the Lower Cretaceous Manniville Group in the study area. Based on the information presented by Wood (1990).

The Glauconitic valley fill channels are 2 -2.5 km wide and up to 30 m thick in the study area (Wood et al, 1989). They cut down through the Calcareous Member to the top of the Sunburst Member. The sandstone bodies contained within the channel are 3-4 km long, 300-500 m wide and up to 22 m thick and they form elongate pods (Wood et al, 1989).

PHYSICAL MODEL

To construct a physical model of the study area sonic velocity information and thickness had to be determined for the different members in the Manniville Group. This information was obtained from the examination of about a dozen well logs from the study area. For the model construction the thickness of the Manniville Member which forms the top of the model and the thickness and velocity of the Mississippian were not important as the zone of interest in the model is the channel and the surrounding members

TABLE 1 MATERIALS AND PARAMETERS USED FOR THE PHYSICAL MODEL

FIELD			MODEL		
FORMATION	AVERAGE P-WAVE VELCITY (m/s)	THICKNESS (m)	MATERIAL	SCALED VELOCITY (M/S)	THICKNESS (m)
MANNVILLE	3500- 3600	-	PLEXIGLAS	3850	178
GLAUCONITE	3370	4-16	TRABOND	3600	10.78
OSTRACOD	4719	2.5-4	TRABOND + 0.66 MM GLASS BEADS	4595	4.62
BANTRY	2748	2.5-7	LEXAN	3016	5.53
SUNBURST	3846	18-37	PLEXIGLAS	3850	88
MISSISSIP-PIAN	5400	-	ALUMINUM	8904	44.45
CHANNEL SAND	2900	30	PLASTER OF PARIS	3045	30
CHANNEL SHALE	4166	30	POLYESTER RESIN + 0.1 MM GLASS BEADS	4070	30

A physical model was constructed of a meandering channel system with a 630 m wide channel and a 320 m wide point bar (Figure 2). The model was constructed using a 1:7000 distance scale factor. This value was chosen as it produces a reasonably sized channel at the model scale for a world scale 630 m wide channel.

To construct the physical model a material had to be found for the channel point bar that was moldable and was porous so it could simulate the channel sand bodies. Plaster of Paris was chosen as the material of choice for the point bar because it was shapeable both wet and dry and it has high porosity so it can simulate a sand point bar. The P- wave material velocity of Plaster of Paris is 2175 m/s so to make Plaster of Paris simulate the point bar a scale factor of 1:1.333 would be required. The time scale factor for the model is calculated from the following equation .

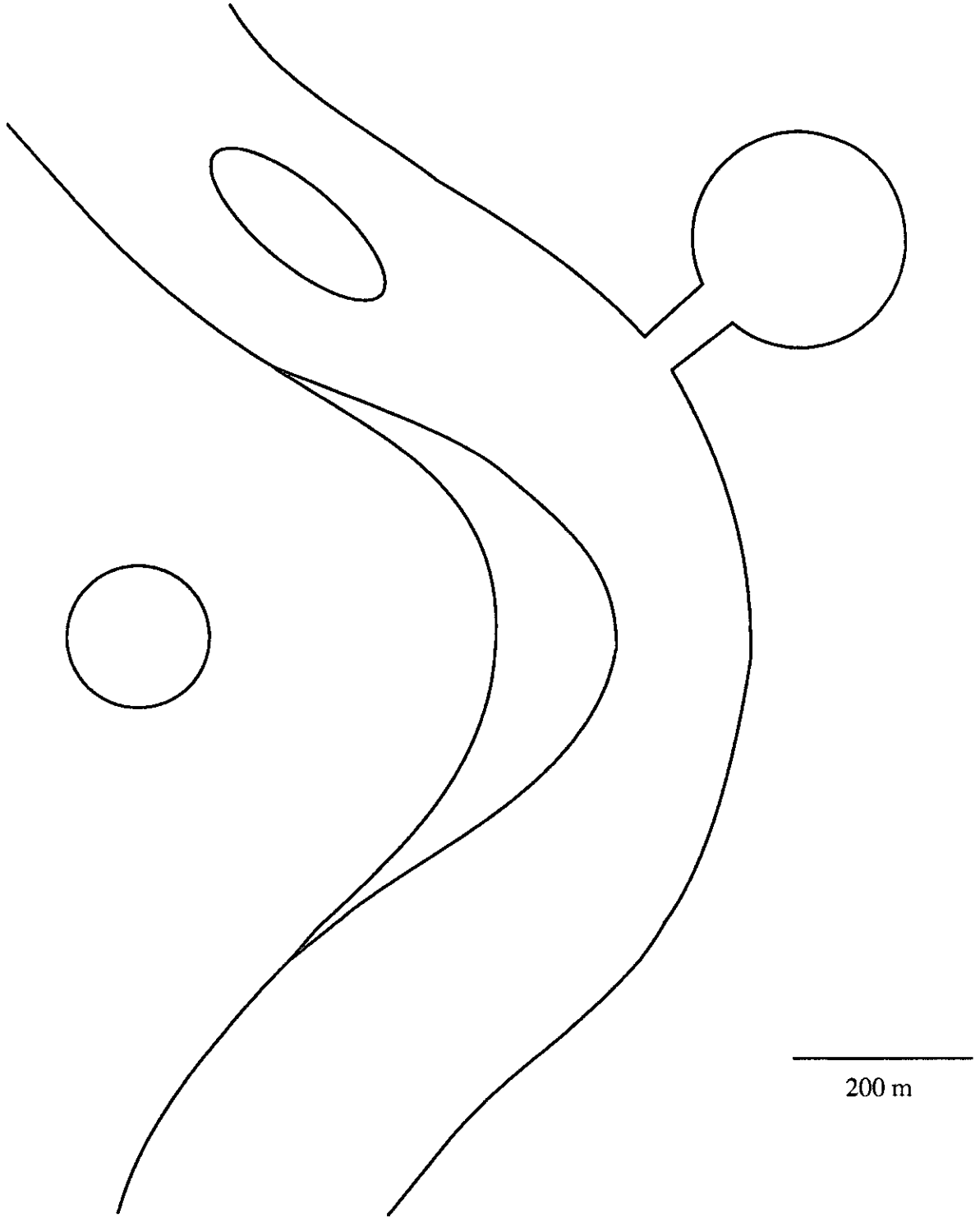

FIG. 2. Schematic diagram of the physical model.

$$1)\ \text{Velocity} = \frac{\text{Distance}}{\text{Time}}$$

$$\therefore\ \text{Time} = \frac{7000}{1.33} = 5250$$

A scale factor of 1:5250 is not possible for the physical model acquisition system so the time scale factor was changed to 1:5000 which produces a velocity scale factor of 1:1.4 for the physical model.

It was decided to include the Cutbank Member in the Sunburst Member for the physical model construction as their velocities are very similar. Various materials were tested and the materials shown in Table 1 were used to simulate the different formations in the physical model.. Aluminum was used to simulate the Mississippian formation even though its scaled velocity is much higher than the Mississippian formation because a stiff base was required to prevent flexure of the model. A cross section through the center of the point bar is shown in Figure 3.

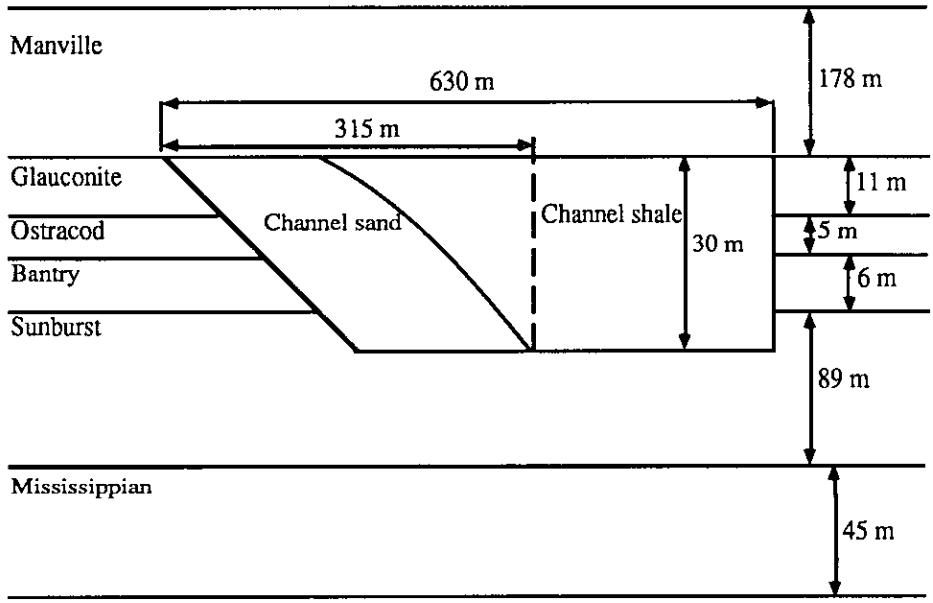

FIG. 3. Cross section through the point bar.

3-D ACQUISITION PARAMETERS

To determine the proper acquisition parameters for a 3-D seismic survey over the model both Seismic Image Software's FDTOOLS and FD33 software was used. The FDTOOLS software provides raytracing of a user input model to determine the source-receiver offset that is required to image the zone of interest on the user input model. This software was used to determine the source-receiver offset which is required to image a geological model consisting of a 1000 m wide channel at a depth of 1000 m. The model which was input into FDTOOLS had P-wave formation velocities similar to the study area. It was found from this program that a offset range of at least

1000 m was required to image a 1000 m wide channel. This is an offset/depth ratio of 1.0. It was decided to use a 25 x 25 m bin size in the 3-D survey because this would provide a minimum of 12 bins over the 315 m wide point bar in the model. The bin size was fixed at 25 x 25 m and the source receiver offset was set at a minimum of 1000 m.

The FD33 software produces subsurface and surface fold coverage diagrams, and calculates source-receiver azimuth and offset distance for various source line, receiver line and source/receiver spacing Various shooting strategies were tried using the FD33 software to determine a reasonable fold coverage and azimuth and offset distribution for the 3-D seismic survey. The shooting strategy that is used by FD33 consists of a user defined receiver patch that is either rectangular or circular. A rectangular patch was used in all the shooting strategies for this study and it was created by defining the number of receiver lines and the number of receivers to be used for each shot in the 3-D survey. The shooting pattern for each strategy is such that each of the shots in the first source line are shot sequentially then the second source line is shot sequentially from the opposite end of the line compared to the first source line. The shots in each source line are shot sequentially with the opposite shooting direction on each alternating source line. The FD33 software shoots four shots into each receiver patch before it begins to roll the receiver patch along increasing the receiver patch by one receiver line after each four shots. This pattern repeats till the receiver patch contains the maximum number of receiver lines that the user has defined for each receiver patch. Then the whole receiver patch will shift by one receiver line after each four shots are fired into a receiver patch. This pattern continues till the receiver patch reaches the edge of the survey where roll-out begins. Once four shots have been fired into a receiver patch, the receiver patch then moves up by one receiver line and any receivers which lie beyond the edge of the survey are deleted. This continues until all the shots on each source line have been fired. The receiver patch is set up such that the first shot fired into a receiver patch is always in the center of the receiver patch.

The first shooting strategy consisted of a 4000x4000 m survey with a 200 m receiver line spacing, 400 m source line spacing and a 50 m source and receiver station spacing. The receiver patch consists of 9 receiver lines and 40 receivers per line The source lines lie in the E-W direction while the receiver lines are N-S. A patch move of 50 m E-W and 400 m N-S was used. Therefore each source fires individually into each receiver patch and each source is only fired once. If the E-W patch move was made to be a 100 m then two sources would fire simultaneously into each receiver patch. The subsurface fold coverage for this survey was calculated using an offset range from 0 -1500 m (see Figure 4). This shooting strategy produces a checkerboard distribution of subsurface fold coverage. There are lines of alternating rectangular zones of 8 and 10 fold coverage between the source lines and along the source lines there is alternating rectangular zones of 12 and 15 fold coverage. It was found that if the number of receivers per line in the receiver patch multiplied by the receiver station spacing and divided by the source line spacing was not an even integer then there would be low bands of fold coverage in the survey. It was also found that if the number of receiver lines per patch multiplied by the receiver line spacing and divided by the E-W patch move was not equal to an even integer then there would be low bands of different fold coverage in the survey. If either of these two options were not met then there would be bands of low fold coverage in the survey. If option one is not met then there is an odd number of source lines contained in each receiver patch and this produces the low fold coverage bands For this survey option one is not met and this could explain the strange fold coverage that occurs in this survey.

The next shooting strategy used the same survey size, source and receiver line spacing and station interval as strategy 1. The receiver patch was decreased in size to 30

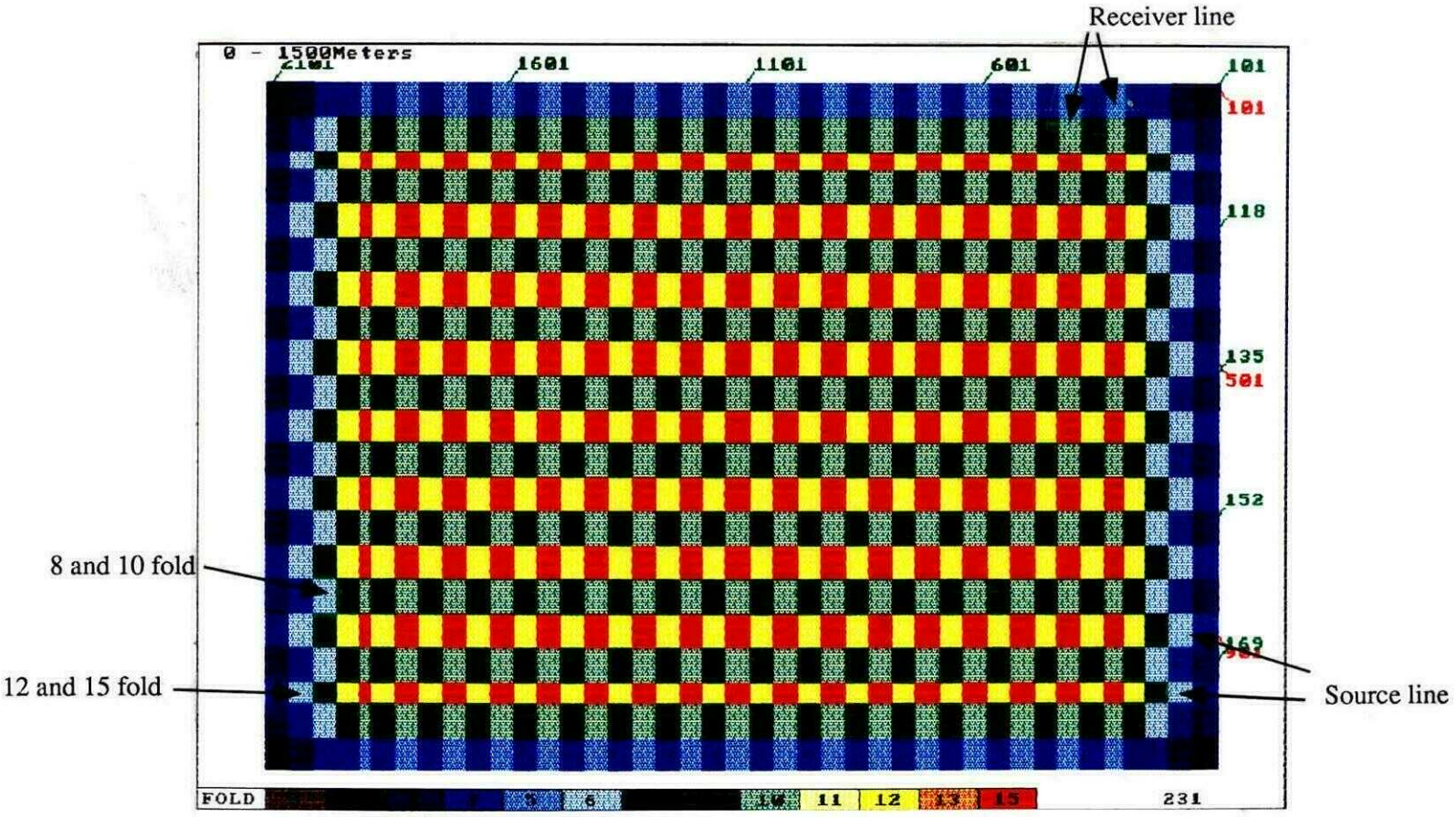

FIG. 4. Strategy 1 Subsurface fold coverage

receivers per line and 8 receiver lines. The subsurface fold coverage for this survey was calculated using an offset range of 0-1500 m (Figure 5). The fold coverage is fairly consistent over the survey at about 8 fold but there is still some bands of low fold coverage (4 fold) along the source lines. For this survey option 1 is non integer so there is an odd number of source lines per receiver patch

The third shooting strategy used the same survey set up as strategy one but the receiver patch was enlarged to 48 receivers per line and 10 receiver lines. For this strategy both options 1 and 2 are met so there should be no problem with bands of low fold coverage for this strategy. The subsurface fold coverage was calculated for this strategy using an offset range of 0-1500m (Figure 6). There is a consistent fold coverage of 15 fold throughout the center of the survey. The offset distribution was also calculated for this strategy and it indicates the maximum offset for this strategy is 1250 m. the offset distribution is well distributed in each of the bins. Figure 7 shows the offset distribution in some of the bins in the center of the survey. The azimuth distribution was also calculated and Figure 8 shows the azimuth distribution in some of the bins in the center of the survey. The star shaped azimuth distribution in each bin indicates that there is a full 360 degree range of azimuths in the bins in the center of the survey area.

This strategy meets all the requirements for the 3-D survey but a problem is that there are to many traces in the survey so that the acquisition time for this survey would be too long. This survey was modified by decreasing the number of source lines and receiver lines in the survey while maintaining the same receiver patch of 10 receiver lines and 48 receivers per line. The survey size was reduced so there were only 7 source lines and 10 receiver lines in the survey. The survey was further modified by deleting source points at each end of the source lines and deleting receivers which lay beyond the edge of the grid produced by the source lines (Figure 9). These modifications to the survey reduced the number of traces recorded in the survey to approximately 70000, reduced the center of the subsurface fold coverage to 14 and reduced the area of 14 fold to a rectangle of 1100 m E-W by 1600 m N-S. The full fold coverage zone for this strategy is sufficiently large that the 3-D seismic survey shot in the modeling tank will have full constant fold over the channel surrounding the point bar including the channel splay and approximately half the lateral bar.

2-D DATA ACQUISITION, PROCESSING AND INTERPRETATION

A 2-D high spatial resolution line was shot perpendicular to the point bar crossing through the center of the point bar. This line was shot for two reasons. The first reason was to provide a high quality channel and point bar signature. The second reason this line was shot was to evaluate a theory determined by Noah (et al, 1991) that sideswipe energy from the out of plane sand body affects the amplitude of events on the 2-D seismic sections and this makes it difficult to determine variation in the thickness of the sand body.

A 2-D high resolution survey was acquired over the model using the University of Calgary's physical modeling tank. The acquisition parameters for this survey are indicated in Table 2.

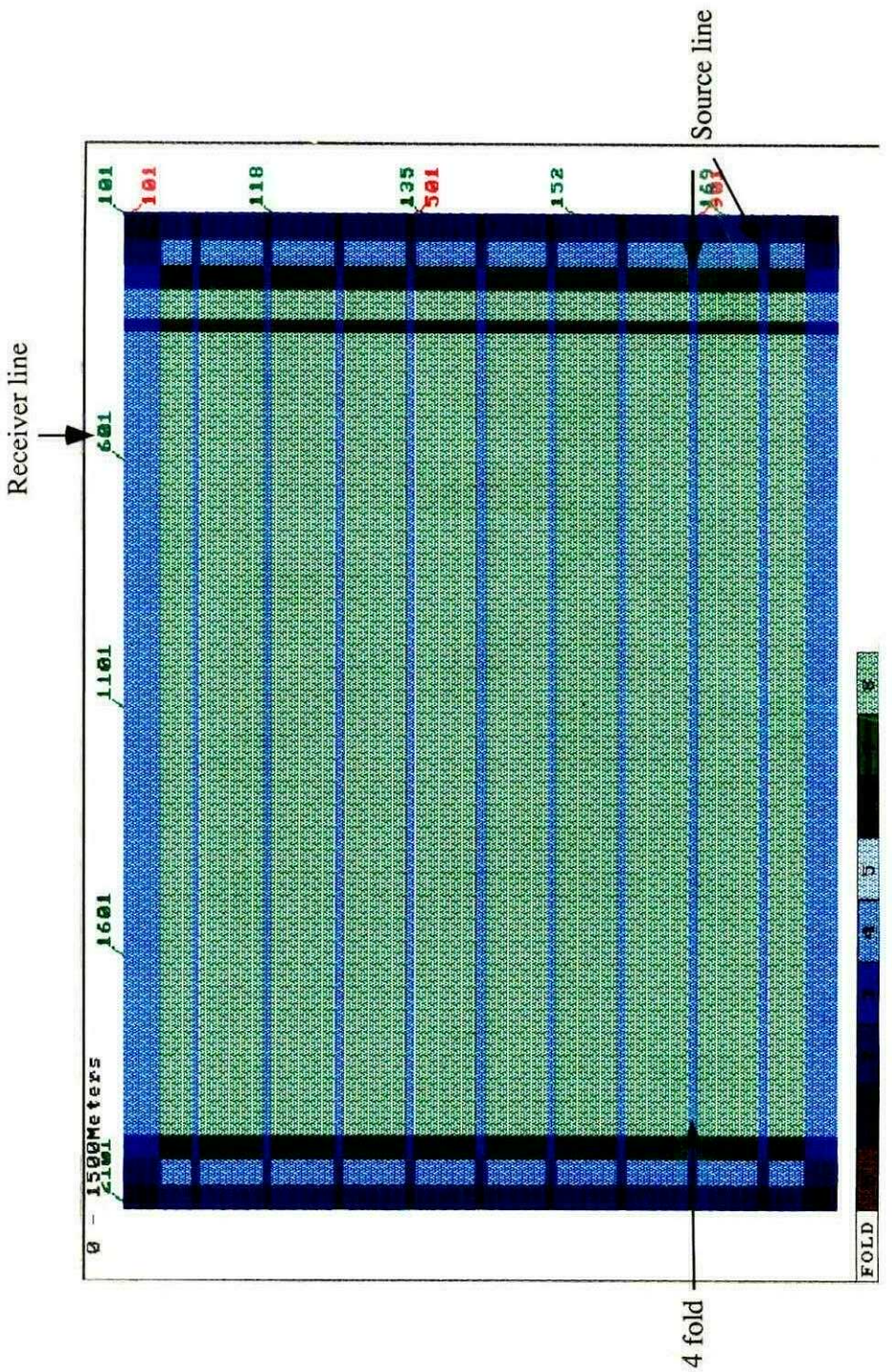

FIG. 5 Strategy 2 subsurface fold coverage

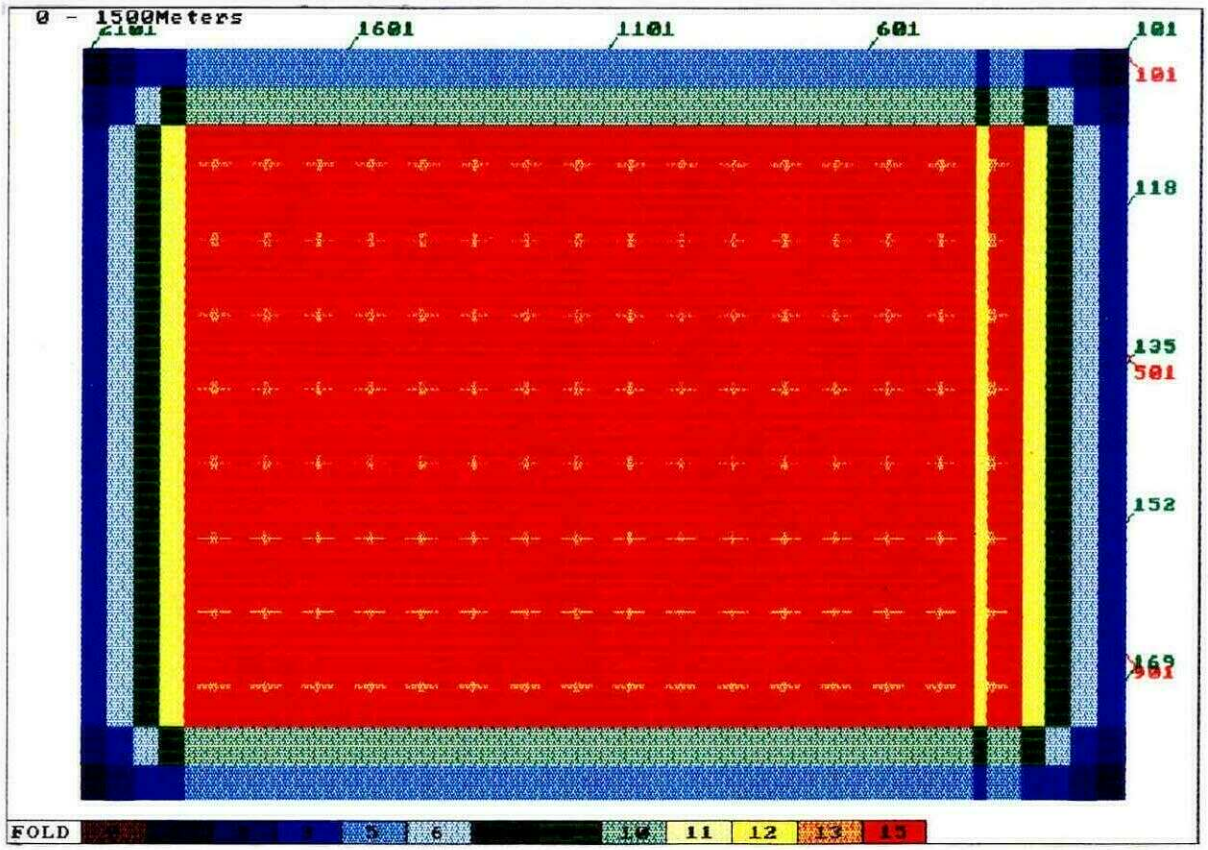

FIG. 6. Strategy 3 Subsurface fold coverage

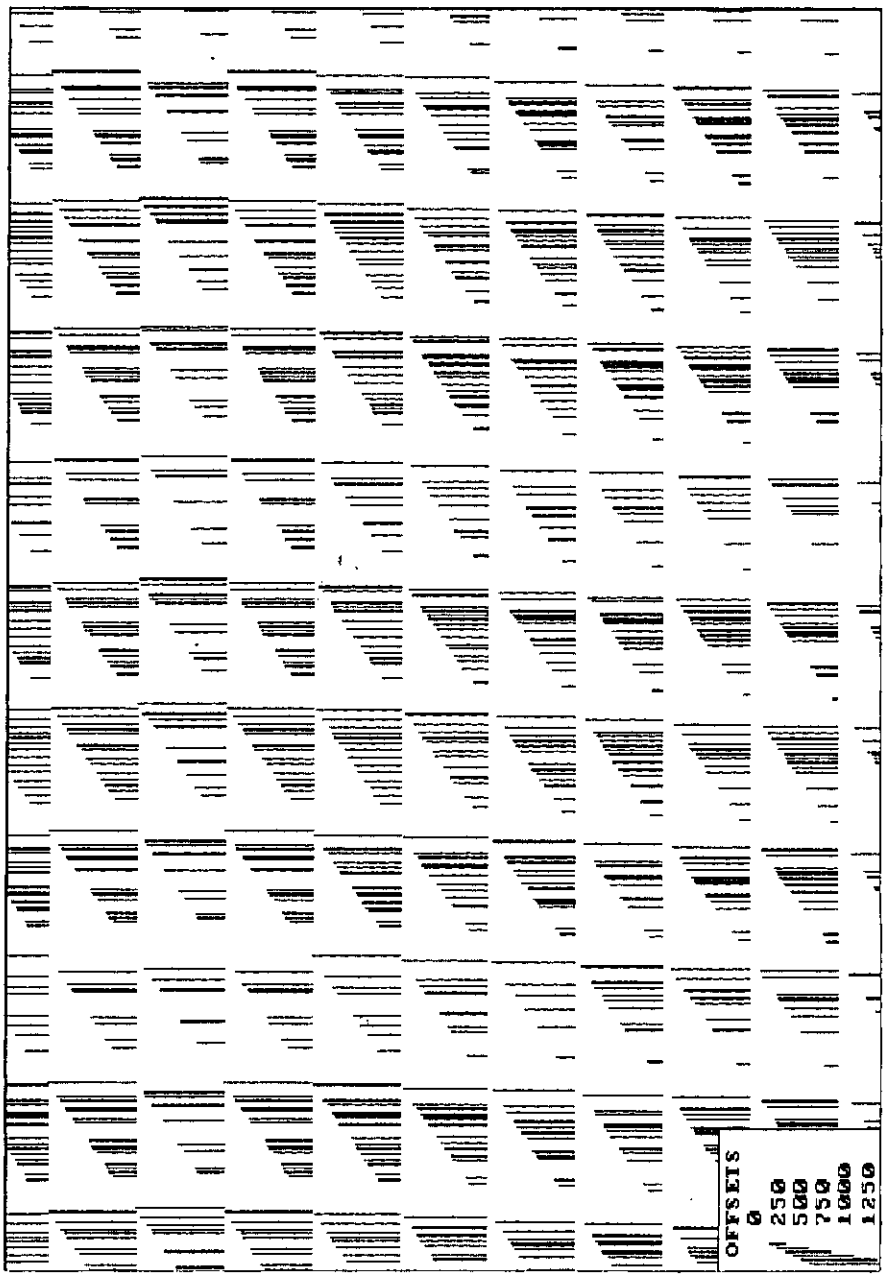

FIG. 7. Strategy 3 Offset distribution

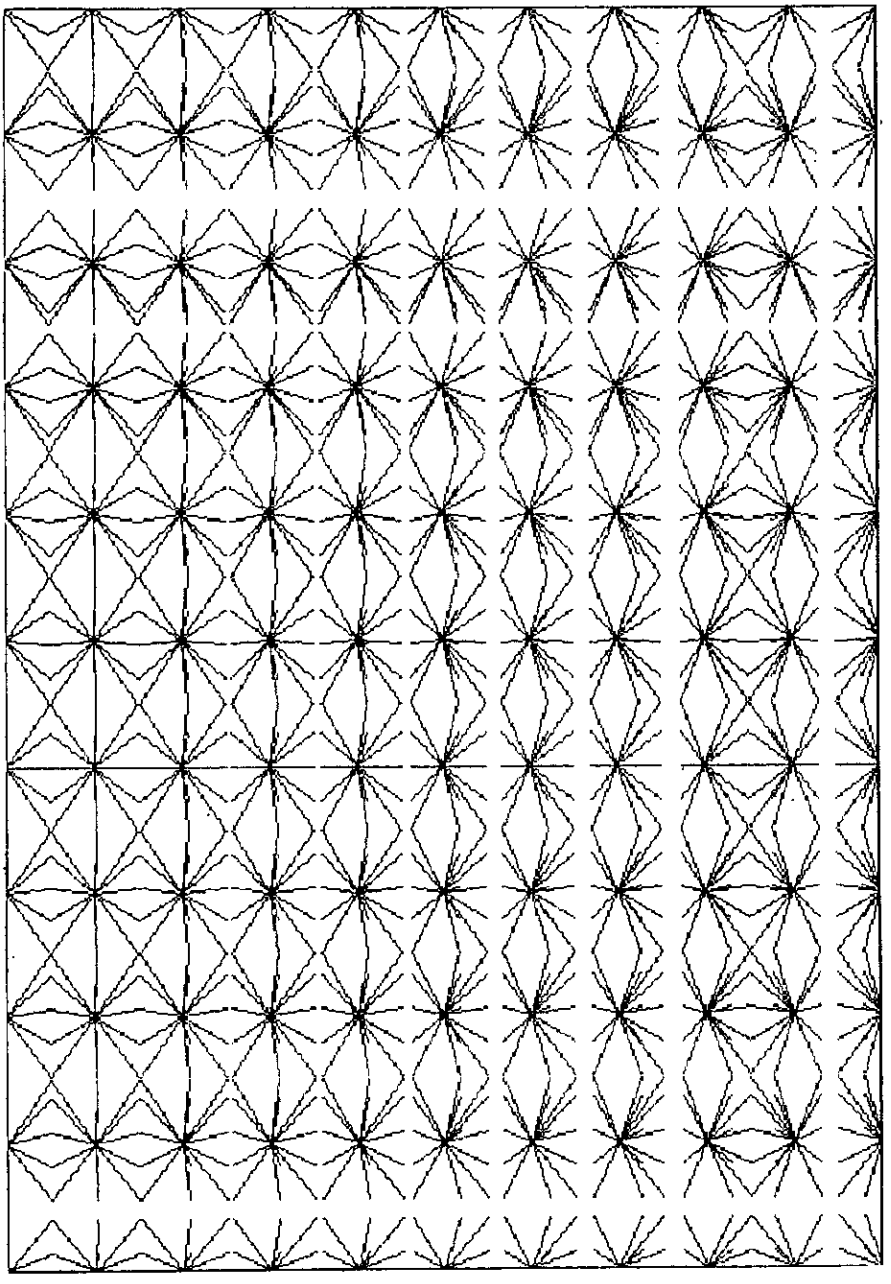

FIG. 8. Strategy 3 Azimuth distribution

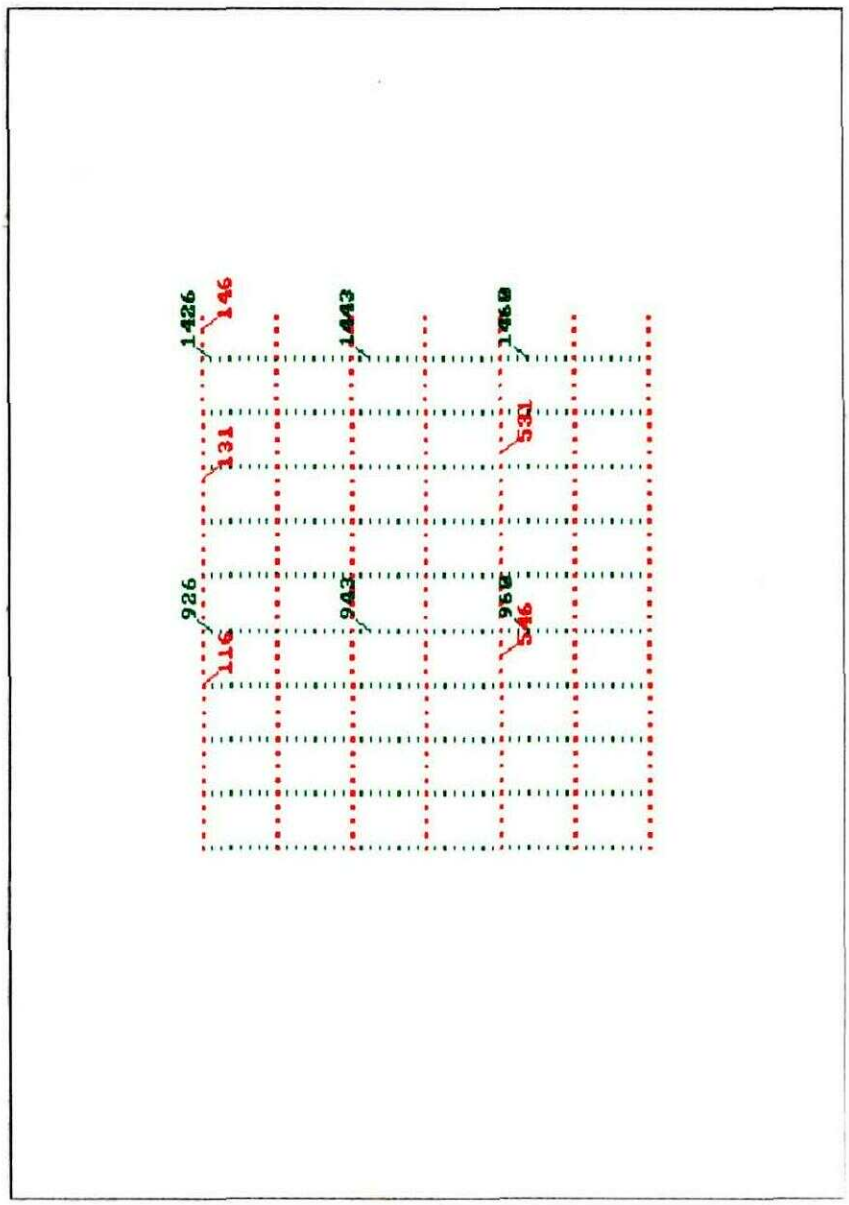
1426
146
1443
1468
531
131
926
943
952
546
116

TABLE 2 2-D DATA ACQUISITION PARAMETERS

21 m station interval

63 m shot intervals

120 trace split spread geometry

105 m near offset

1344 m far offset

Data processing

A standard processing flow (Figure 10) was used to process the 2-D data. Once the data was stacked a time variant scaling factor was applied to the final display of the stacked section (Figure 11). This type of scaling factor was needed to boost up the strength of the reflections between the top of the Manniville (Plexiglas) and the top of the Mississippian (aluminum). Normal incidence reflections coefficients were calculated for all of the interfaces in the physical model and it was found that the top of the Mississippian, top Bantry, top Manniville have strong reflection coefficients while the rest of the layers have very weak reflection coefficients. The final stacked sections were post-stack time-migrated using f-x migration, finite-difference migration and a phase-shift migration (Figures 12,13 and 14).

Data interpretation

The top of the Manniville is at approximately 0.92 s on the stacked section (figure 10). It is a fairly strong amplitude peak with good continuity across the section. The next obvious events on this section are the peak and strong trough doublet that occurs at 1.015 s and 1.02 s which represent the Ostracod limestone and the Bantry shale. There is a weak peak directly below the Bantry trough which represents the top Sunburst formation. The strong peak at 1.085 s represents the top of the Mississippian event. The strong trough of the Bantry shale and weak Sunburst peak disappear at approximately trace 125 on the stacked section. This disappearance of this trough peak doublet indicates the start of the channel on this section. This disappearance of this trough peak doublet also corresponds to a strong pull-up on the Mississippian event caused by the high velocity channel shale. There is a slightly dipping event occurring

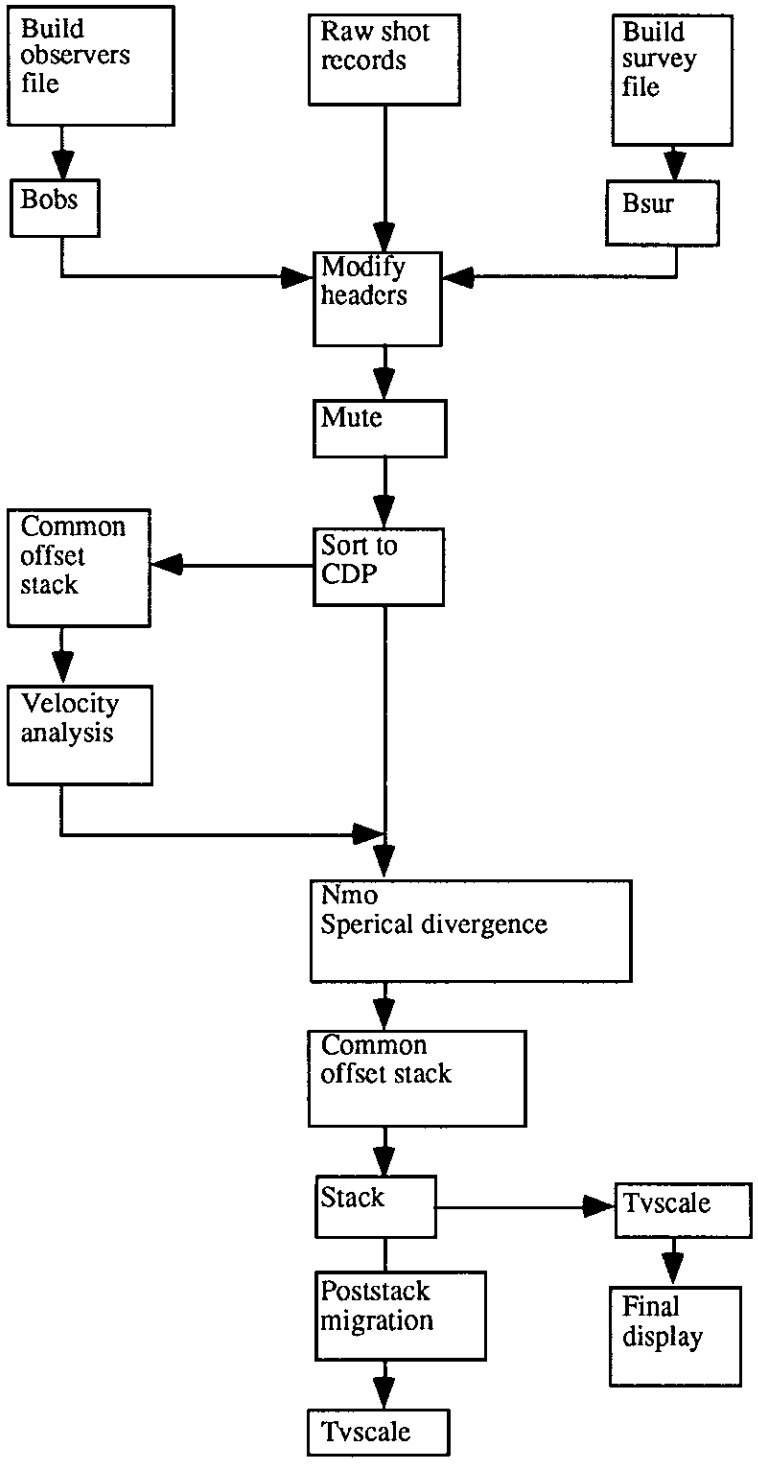

FIG. 10. 2-D processing flow

between 1.01 and 1.03 s, starting on trace 164 to 180, which represents the top of the point bar. This event appears to level out at 1.005 s at trace 180 and it can be followed along to trace 194 where it appears to merge into the Ostracod event. The dipping event below the top of the point bar probably represents the dipping inside edge of the

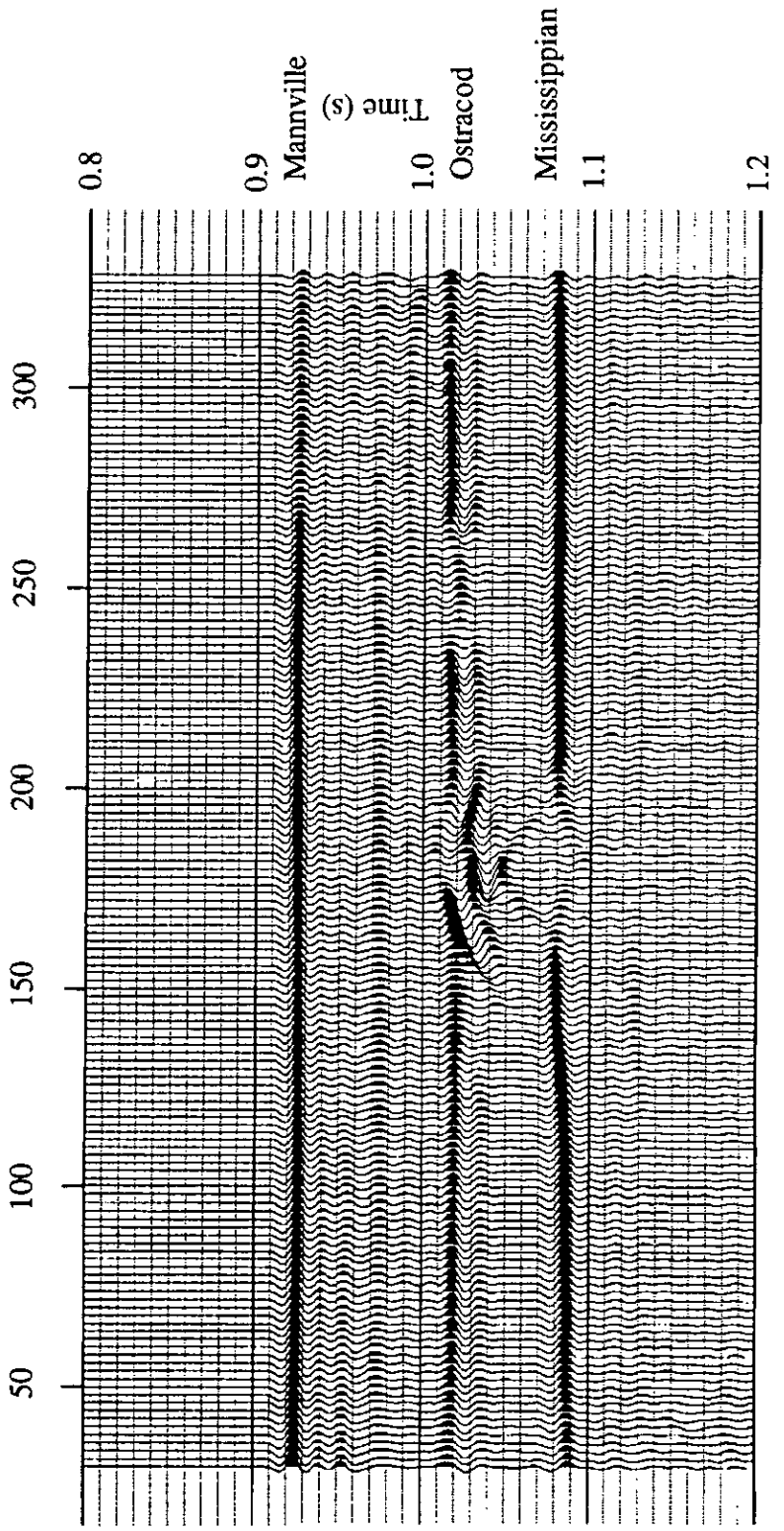

FIG. 11. Stacked section

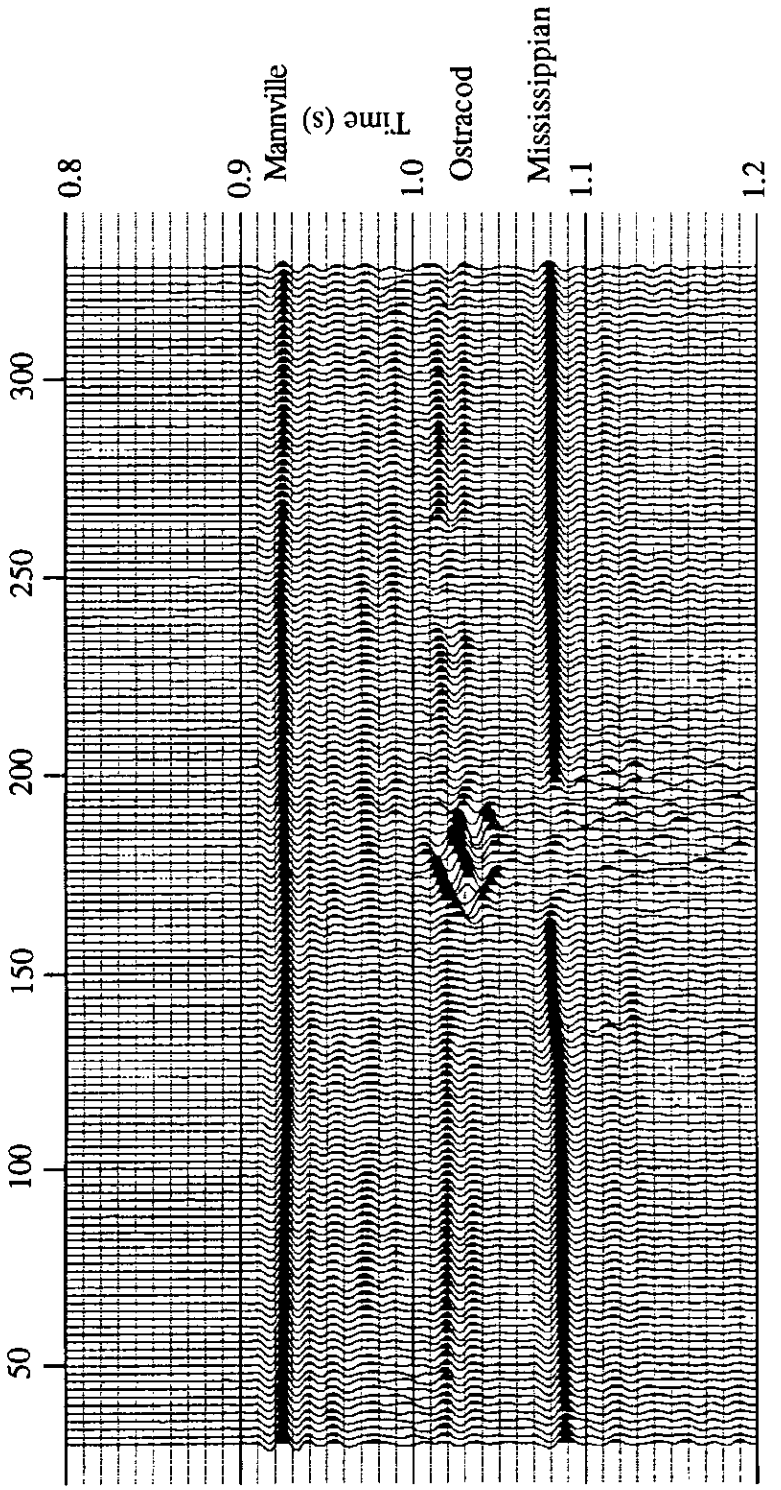

FIG. 12. F-x migrated section

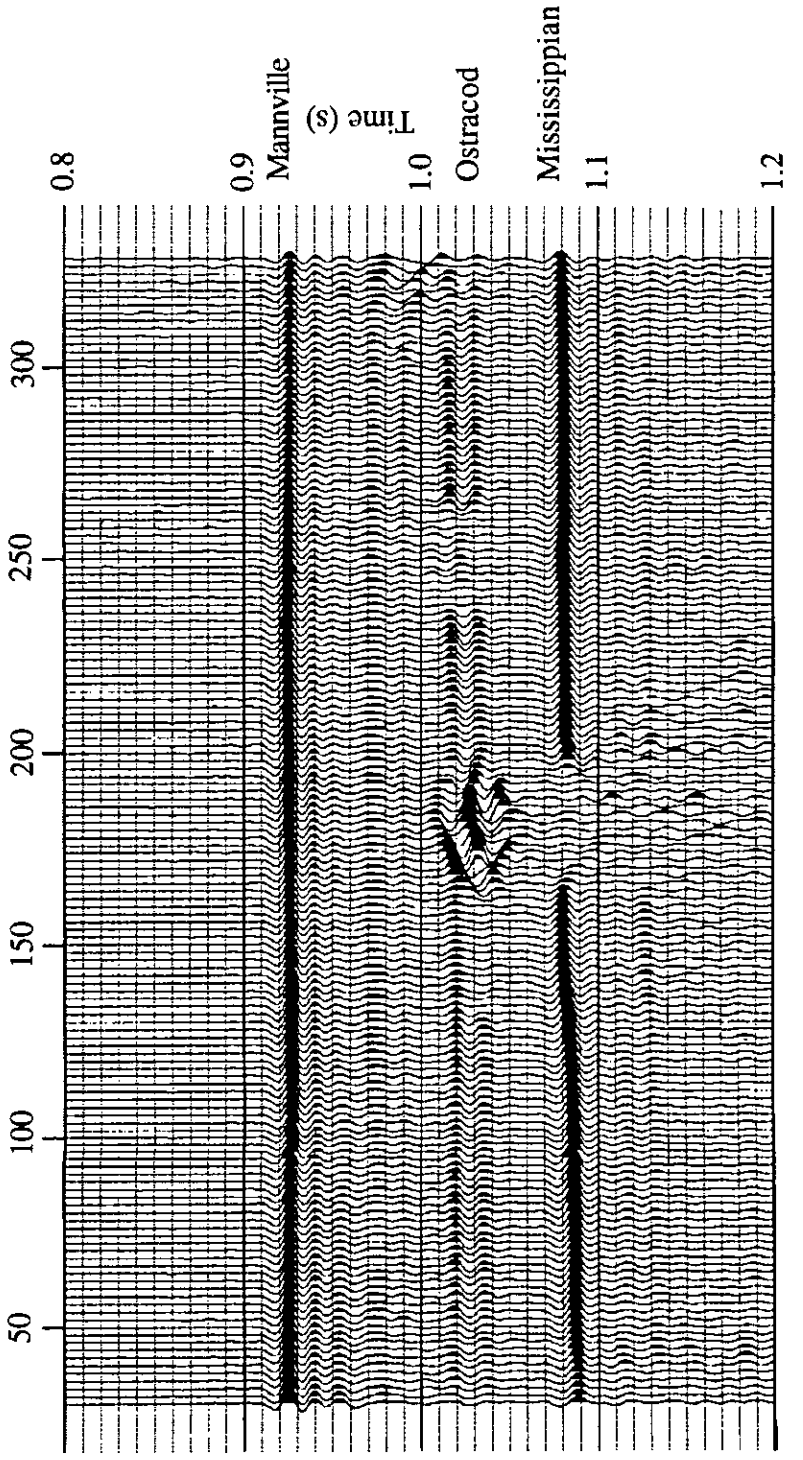

FIG. 13. Finite-difference migrated section

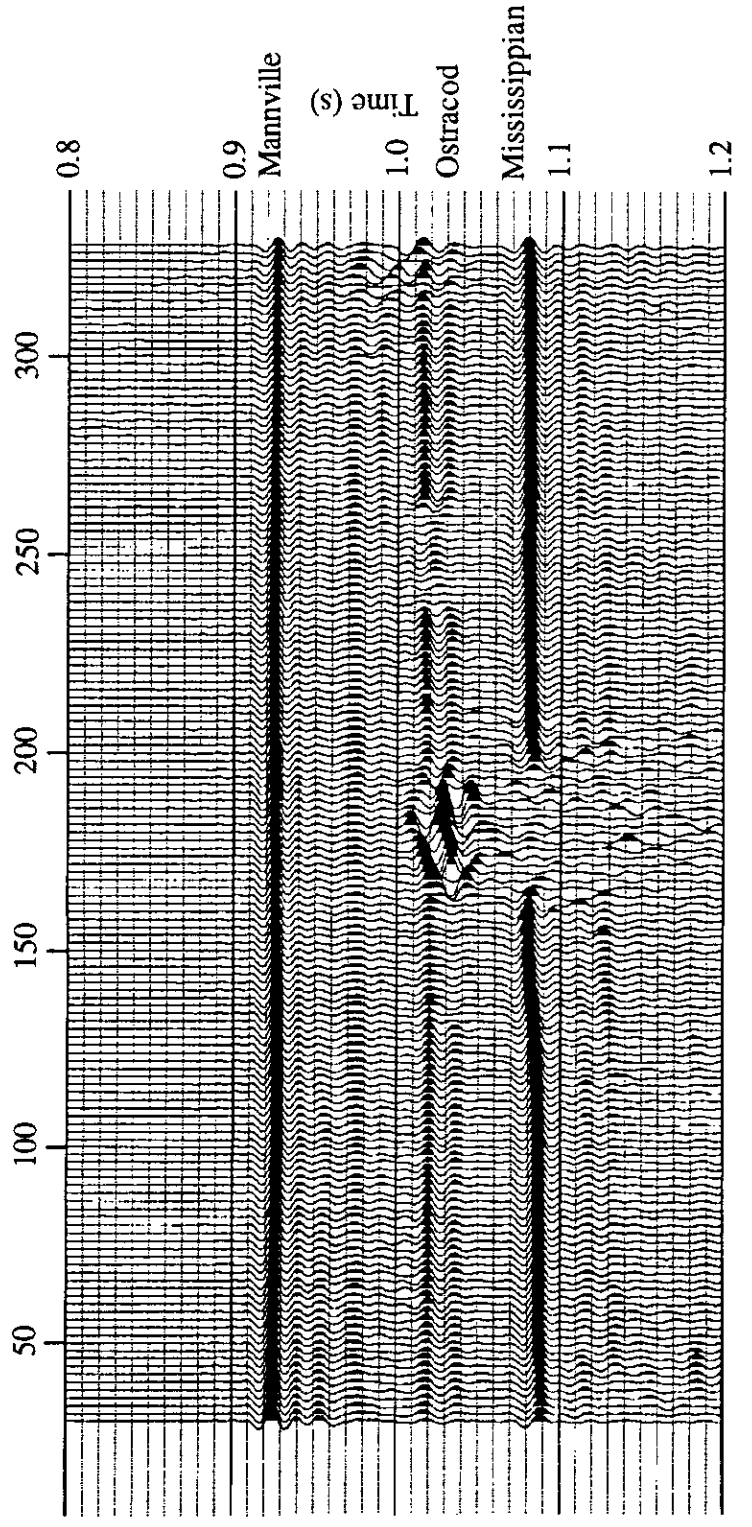

FIG. 14. Phase-shift migrated section

channel. The point bar seems to attenuate all the energy passing through it so there appears to be a break in the Mississippian reflector below the point bar and there are diffraction's produced off each side of the break.

The three time-migrated sections have very similar appearances. Each migration has collapsed the diffractions which occur in the channel on the unmigrated stacked section. Each of these sections also has a slight hint of a diffraction on the left side of the break in the Mississippian event. This may be caused by the lateral variation in the velocity in the channel above as the point bar increases in thickness. These migration routines may have trouble dealing with this lateral velocity variation in the channel. The finite-difference and phase-shift migration seem to image the top flat part of the point bar better than the f-x migration. It is possible on the finite-difference and phase-shift migrated sections to follow the point bar reflection up the front slop of the point bar and across the flat top of the bar. The reflection from the top of the bar then merges with the Ostracod event on these two sections. The f-x migrated section only images the front slope of the point bar with only a hint of a reflection from the top of the point bar.

A second major difference in these migrations is the amount of time each algorithm takes to produce a migrated section. Using the same input data set the phase-shift migration migrates the data in approximately 1.5 minutes while the f-x migration takes about 7 minutes and the finite-difference migration takes approximately 30 minutes. These times are all based on running each of the migrations on a Sun SPARCstation 2 .

There appears to be no change in the amplitude of the dipping reflection on either the migrated or unmigrated sections as the point bar thickens from zero thickness to 30 m. This observation seems to reinforce the observation made by Noah (et al, 1991) that the sideswipe energy is so strong that there is no variation in reflection amplitude from the point bar as the bar varies in thickness.

3-D ACQUISITION

A full 3-D survey was acquired over the model using the University of Calgary's physical modeling tank. The survey was acquired using the modified third shooting strategy described above. The data was acquired in such a way that the source was always located in the center of the receiver patch. The data was also acquired in such a way that any receivers which lay outside of the grid formed by the source lines were not recorded. Therefore the first three source lines and the last three source lines in the survey each had receiver patches which went beyond the source grid so these receiver positions were not recorded. This acquired data was shot in the physical modeling tank and it was stored on the Perkin Elmer computer system. The data was then transferred to the Sun workstation where it is being processed using ITA's 3-D software. A shot gather from the survey is shown in Figure 14 which has had a flat mute applied to remove the direct arrivals.

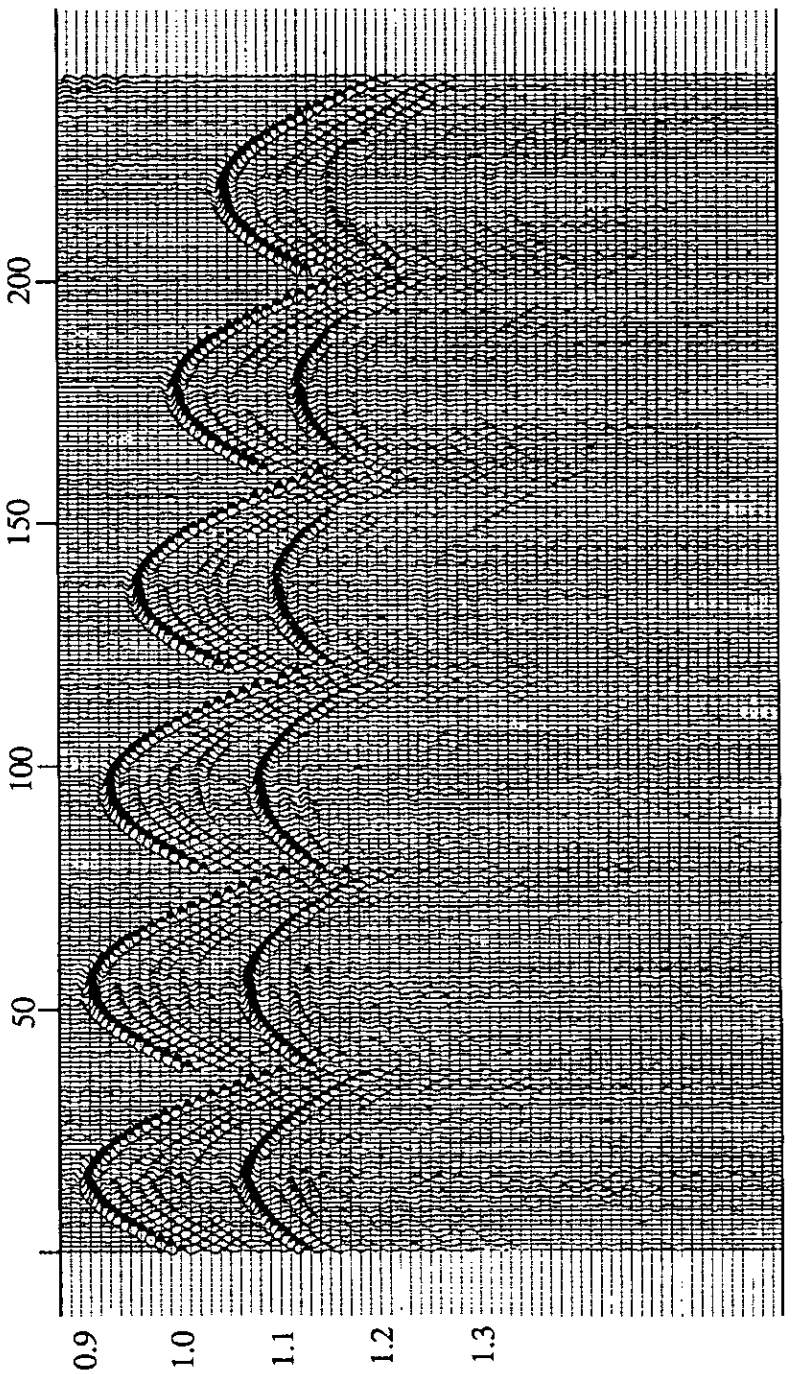

FIG. 14. Raw 3-D shot record

CONCLUSIONS

The first conclusion that can be drawn from this study is that variation in the receiver patch can have a tremendous effect on the subsurface fold coverage and distribution. The survey set up was the same for each of the 3 shooting strategies used in the 3-D acquisition tests, but the subsurface fold coverage and distribution for each test varied widely.

A second conclusion is that the different post-stack 2-D migrations produce comparable migrated sections for the 2-D data set. The difference between them is in the amount of time it takes each migration to produce the migrated section. The phase-shift migration is the fastest with the f-x migration being about 5 times slower than the phase migration and the finite-difference migration been approximately 20 times slower than the phase migration.

The third conclusion is that sideswipe energy from the out of plane sand body is so strong that it masks any variation in amplitude of the reflection from the point bar as the point bar varies in thickness.

The final conclusion is that the point bar appears to attenuate high frequencies so it tends to produce a shadow zone on the reflectors below the point bar. This may be helpful for identification and interpretation of shallow point bars.

FUTURE WORK

Possible future work includes the application of a deconvolution operation to the 2-D processing flow to try to collapse some of the ringing in the section produced by a slightly ringy wavelet during acquisition of the 2-D data set. The full 3-D data set will be processed to a stacked 3-D data volume and some AVO analysis will be performed on the data set to see if 3-D AVO analysis is a viable option for identification and interpretation of point bars in a meandering stream environment.

ACKNOWLEDGMENTS

We would like to thank Eric Gallant for his help in building the physical model and data acquisition and Mark Lane for his help and suggestions in processing the data

REFERENCES

Hopkins, J. C., Hermanson, S. W., and Lawton, D. C., 1982, Morphology of channels and channel-sand bodies in the Glauconite Sandstone Member (Upper Mannville), Little Bow Area, Alberta: Bulletin of Canada Petroleum Geology, v. 30, p. 274-285.

Noah, J. T., Hofland, G., and Lemke, K., 1991, Seismic interpretation of meander channel point-bar deposits using realistic seismic modeling techniques: 6th Ann. Internat. Mtg., Soc. Expl. Geophy., Expanded Abstracts, 210-212.

Wood, J. M., 1990, Sequence stratigraphy, Sedimentology and petroleum geology of the Glauconitic Member and adjacent strata, Lower Cretaceous Mannville Group, southern Alberta: PhD thesis, University of Calgary, v. 1, 355 p.

Wood, J. M., and Hopkins, J. C., 1989, Resevoir sandstone bodies in estuarine valley fill: Lower Cretaceous Glauconitic Member, Little Bow Field, Alberta, Canada: AAPG Bulletin, v. 73 p. 1361-1382.